High-resolution optical spectroscopy of radio Broad Absorption Line quasars

F. Jiménez-Luján, J.I. González-Serrano and C.R. Benn

Abstract We present high-resolution optical spectroscopy of several high-redshift BAL (Broad Absorption Line) quasars: 0844+0503, at redshift $z = 3.3465$, which has a known radio counterpart observed by the VLA FIRST survey; 0908+0658, at redshift $z = 3.0734$, with no radio detection recorded in the NASA/IPAC Extragalactic Database (NED); and 0217-0854, at redshift $z = 2.5720$, which also has a known radio counterpart observed by the VLA FIRST survey. They show velocity structure on a scale smaller than the separations of the two components in prominent doublets (CIV, SiIV, NV). Comparison of the residual intensities in the two components has allowed us to measure the covering factor and the column densities of several atomic species in the absorbing gas. From these, the ionisation parameters have been measured, providing constraints on the distance of the gas from the nucleus. Kinetic luminosities will be determined (through the distances estimates for plausible assumed values of electron densities) in order to know their impact on the properties and evolution of these quasars and the intergalactic medium.

F. Jiménez-Luján
Dpto. de Física Moderna, Univ. de Cantabria, Avda de los Castros s/n, E-39005 Santander, Spain and Instituto de Física de Cantabria (CSIC-Universidad de Cantabria), Avda de los Castros s/n, E-39005 Santander, Spain, e-mail: jimenezf@ifca.unican.es

J.I. González-Serrano
Instituto de Física de Cantabria (CSIC-Universidad de Cantabria), Avda de los Castros s/n, E-39005 Santander, Spain, e-mail: gserrano@ifca.unican.es

C.R. Benn
Isaac Newton Group, Apartado 321, E-38700 Santa Cruz de La Palma, Spain, e-mail: crb@ing.iac.es

1 Introduction

Broad Absorption Line (BAL) quasars are characterised by extended absorption troughs in the blue wings of ionised UV resonance emission lines. These absorption profiles are thought to be a direct consequence of outflowing gas spatially connected with the central quasar at velocities up to ~ 0.2 c ([9]). In order to classify these objects, we measure the BALnicity Index (*BI*, [13]). In addition, the intrinsic Absorption Index (*AI*, [7]) can be measured so that we can take into account not just broad intrinsic absorption lines but all intrinsic absorption lines. We follow mainly three lines of investigation in order to understand the BAL phenomenon: (i) Orientation vs. Evolution: It is still unknown whether BALs arise in a physically distinct population of quasars ([11]) or whether they are present in most quasars but are intercepted by only $\sim 10-20$ % of the lines of sight to the quasar ([13]), or perhaps none of these contributions can be neglected. (ii) Line-locking effect: An exhaustive study of this effect in our samples will provide us information about the mechanism responsible for the acceleration of the outflows. Absorption-line locking can occur when line-of-sight absorption in one transition blocks photons that would otherwise be absorbed by a second, decreasing the radiation pressure associated with the second transition ([10]). (iii) Covering factors & column densities determination: In order to determine the global properties and the composition of the intergalactic medium, we analyse the spectra of the quasars observed in the optical range with high-resolution. A study of intrinsic Narrow Absorption Lines (NALs) and mini-BALs presented in these BAL quasars will help us to analise the abundances and physical conditions in outflows close to the nuclei of quasars ([5]). As described e.g. in [3], we can analyse doublet lines for which the true ratios are known and compare the observed ratios to the true ratios in order to disentangle the contributions of covering factor and optical depth to the absorption feature. An apparent column density per unit velocity can be derived as described in [12]. Distances of the absorbers to the nucleus, and consequently, the kinetic luminosities of the outflows, are very important to know the properties and the implications for the evolution of the AGN.

2 Data acquisition, analysis and results

Selection of the samples

The connection between radio and optical activity, which still needs to be understood, requires the comparison between radio-loud and radio-quiet quasar populations ([6]). The targets studied in this work were observed as a part of the International Time Programme (ITP) project *The nature of quasar outflows* (granted for the first semester in 2008), which Principal Investigator (PI) is Dr. Chris R. Benn. The main sample for the ITP project was previosly selected from the SDSS DR4 (Data Release 4, [1]) using the following criteria: (i) magnitude in the r band: $r \leq 19.0$;

(ii) redshift: $2.5 \leq z \leq 4.2$; and (iii) good candidate to have the expected velocity structure in the BAL in the lower-resolution SDSS spectra. In addition, we have selected a sample of 67 BAL quasars from the Sloan Digital Sky Survey Data Release 5 (SDSS DR5, [2]) counterparts of sources detected in the survey FIRST (Faint Images of the Radio Sky at Twenty-centimeters, [4], $S_{1.4\ \mathrm{GHz}} > 1.0$ mJy) from the Very Large Array (VLA, belonging to the National Radio Astronomy Observatory (NRAO)). We firstly selected all the FIRST sources with an SDSS unresolved object in the table *PhotoObjAll*[1] of the DR5 Catalog Archive Server (CAS) within $1.5''$ of the radio position, with redshifts $z \geq 1.7$, with magnitude in the r photometric band $r \leq 19.0$, and specClass 3 and 4. The whole sample consisted of 703 sources. Then, we distinguished BAL and non-BAL quasars by visual inspection of the DR5 spectra. Finally, the radio BAL quasar sample is formed by 67 sources.

Observations and standard reduction

The targets presented here were observed with ISIS (Intermediate dispersion Spectrograph and Imaging System) dual-arm spectrograph mounted on the 4.2 m William Herschel Telescope (WHT). During observing, we monitored the signal to noise in real time from quick-look data reduction with the software IRAF so that we could optimise the exposure time according to the weather conditions. In addition, we previously prepared the selected targets for each night depending on visibility and priority order. The observing details are summarised in Table 1. The radio-loud BAL quasar 0844+0503, at redshift $z = 3.3465$, and the radio-quiet BAL quasar 0908+0658, at redshift $z = 3.0734$, were observed on 2007 Mar 10. The radio-loud BAL quasar 0217-0854, at redshift $z = 2.5720$, was observed on 2008 Jan 6,7. The data were reduced in the usual way, using standard packages in IRAF for the bias subtraction, flat fielding, cosmic-ray removal and wavelength calibration. The wavelength calibration details are summarised in Table 2. The spectral resolution (column 3 of Table 2) was measured from the widths of the sky lines. The root mean square (rms) errors in wavelength calibration are given in column 4 of Table 2. The wavelength calibration is accurate to better than 0.3 $\AA$ at all wavelengths. Spectrophotometric standard stars were observed to perform the flux calibration. Heliocentric and vacuum correction were the final steps in data reduction.

Data analysis and results

The target 0844+0503 ($z = 3.3465$) has a known radio counterpart observed by the VLA FIRST survey. Its magnitude is $r = 17.88$ and the total radio flux density is $7.4\,mJy$. The BALnicity Index (*BI*, [13]) and the intrinsic Absorption Index (*AI*, [7]) were computed with a program developed by us for that purpose from the cited definitions. These are the resulting values: $BI = 9090 \pm 100\,km/s$ and $AI = 10340 \pm 100\,km/s$. In this case, the study becomes more complex because of the blending in the absorption lines. Covering factor C and optical depth τ as a func-

[1] See http://cas.sdss.org/astrodr5/en/help/docs/tabledesc.asp for details.

Table 1 Details of observations for 2007 Mar 10 and for 2008 Jan 6, 7. The columns give: (1) Airmass; (2) Seeing; (3) Dichroic used; (4) ISIS arm; (5) Slit width used; (6) Grating used; (7) CCD (Charged Coupled Device) detector; (8) Central wavelength; (9) Exposure time. The lines (a)–(k) give the configuration that will appear in Table 2. The lines (a)–(c) are the observations for 2007 Mar 10 (target 0844+0503), (d)–(c) are the observations for 2007 Mar 10 (target 0908+0658) and (f)–(k) are the observations for 2008 Jan 6, 7 (target 0217-0854).

	Airmass	Seeing ($''$)	Dichr. (Å)	ISIS arm	Slit ($''$)	Grating	CCD	$\lambda_{cen.}$ (Å)	Expos. (s)
	(1)	(2)	(3)	(4)	(5)	(6)	(7)	(8)	(9)
(a)	1.0–1.3	0.9–1.1	5300	blue	0.8	R1200B	EEV12	4400	2×1800
(b)	1.0–1.3	0.9–1.1	5300	red	0.8	R1200R	RED+	6000	1800
(c)	1.0–1.3	0.9–1.1	5300	red	0.8	R1200R	RED+	7900	1800
(d)	1.0–1.3	0.9–1.1	5300	blue	0.8	R1200B	EEV12	5000	2×1800
(e)	1.0–1.3	0.9–1.1	5300	red	0.8	R1200R	RED+	6250	2×1800
(f)	1.3–1.9	1.0–2.5	5300	blue	1.0	R1200B	EEV12	3915	1800
(g)	1.3–1.9	1.0–2.5	5300	red	1.0	R1200R	RED+	5340	2×1800
(h)	1.3–1.9	1.0–2.5	5300	blue	1.0	R1200B	EEV12	4790	2×1800
(i)	1.3–1.9	1.0–2.5	5300	red	1.0	R1200R	RED+	6490	1800
(j)	1.6	0.5	5300	blue	0.5	R1200B	EEV12	4790	1800
(k)	1.7	0.5	5300	red	0.5	R1200R	RED+	6490	1800

Table 2 Details of wavelength calibration for 2007 Mar 10 and for 2008 Jan 6, 7. The columns give: (1) Central wavelength; (2) Wavelength range; (3) Resolution; (4) The root mean square (rms) errors in wavelength calibration. The lines (a)–(k) give the configuration that appeared above in Table 1. The lines (a)–(c) are the observations for 2007 Mar 10 (target 0844+0503), (d)–(c) are the observations for 2007 Mar 10 (target 0908+0658) and (f)–(k) are the observations for 2008 Jan 6, 7 (target 0217-0854).

	$\lambda_{cen.}$ (Å)	Wavelength range (Å)	Resolution (Å)	σ_{λ} (Å)
	(1)	(2)	(3)	(4)
(a)	4400	3940–4875	0.82	0.04
(b)	6000	5560–6590	0.73	0.07
(c)	7900	7460–8480	0.73	0.16
(d)	5000	4540–5350	0.82	0.12
(e)	6250	5810–6840	0.73	0.18
(f)	3915	3450–4390	0.90	0.03
(g)	5340	4890–5930	0.85	0.3
(h)	4790	4330–5260	0.90	0.13
(i)	6490	6040–7070	0.85	0.10
(j)	4790	4330–5260	0.55	0.12
(k)	6490	6040–7070	0.44	0.06

tion of velocity have been derived for the AlIII BAL spectrum using a program developed by [5]. Although, for AlIII, a value for the column density can be obtained, the complexity for SiIV obliges us to improve this method so that covering factors and optical depths can be recovered even from blended components. The target 0908+0658 ($z = 3.0734$) has no radio detection recorded in the NED (NASA/IPAC Extragalactic Database). Its magnitude is $r = 18.80$. This case is also a complex one because of the blending in the absorption lines again. The target 0217-0854

($z = 2.7520$) has a known radio counterpart observed by the VLA FIRST survey as well. Its magnitude is $r = 18.20$ and the total radio flux density is $5.6\,mJy$. The BI and AI are the following: $BI = 39 \pm 17\,km/s$ and $AI = 3360 \pm 90\,km/s$. The spectra obtained include several complex troughs and some other doublets, as the CIV mini-BAL (blueward the BAL trough), used for determining preliminary results. We have used a modified program (from the previous one, [5]) for the covering factors and the optical depths determination for CIV and SiIV mini-BALs, corresponding to an absorber at $z \sim 2.457$. If we select a range in velocities, e.g. from ~ 10050 to $\sim 10100\ km/s$, we illustrate graphically the error estimate in Fig. 1. Errors on τ and C are estimated by propagation of errors on I_b and I_r (only in the permitted regions). We estimate the ionisation parameter using the results described in [8]. We assume $\sigma_{logU} = 0.2$. As the number of generated photons follows a Poissonian distribution, we estimate the 1σ uncertainties on the residual intensities of both components of the doublet as the square root of this total number of photons. Preliminary results are summarised in Tables 3 and 4.

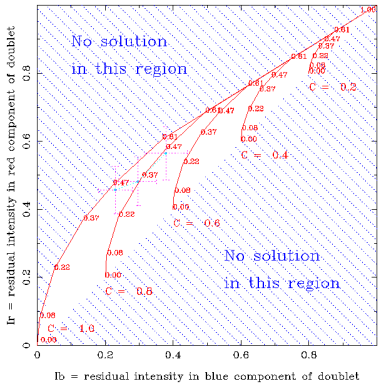

Fig. 1 Derivation of the covering factor C (red numbers in large font) and optical depth τ ($e^{-\tau}$, small font) from the residual intensities I_b and I_r in each component of the CIV doublet line. The light blue curve shows the locus of the derived C and τ in the velocity range selected and the pink error bars show the errors for the residual intensities I_b and I_r (modified program, from the previous one developed by [5])

3 Discussion and future work

As the covering factors were found to be velocity dependent, we can say that BALs are intrinsic absorbers since a surrounding host galaxy or intervening galaxies would completely cover the central source along our line of sight. The orders of magnitude of the distances estimates are consistent with outflows that produce effects on their host galaxies, but it is unlikely to have a significant impact on the intergalactic medium. Their kinetic luminosities will be determined from these estimates. However, they need to be improved, e.g. by obtaining accurate values for the electron density, since distances strongly depend on this parameter. For this purpose, higher resolution spectra have been already obtained for some quasars using VLT UVES and Keck HIRES. The line-locking effect has to be studied in all the candidates ob-

Table 3 Preliminary results for the absorber at $z \sim 2.457$ and in the range $\sim 10050 - \sim 10100\, km/s$ for CIV and SiIV mini-BALs of the target 0217-0854, observed on 2008 Jan 6, 7. The columns give: (1) Ion; (2) Covering factor C; (3) $e^{-\tau}$; (4) Optical depth τ; (5) Column density N for the range $\sim 10050 - \sim 10100\, km/s$ ([12]); (6) $log\, N$. The estimate for the covering factor in the SiIV mini-BAL, $C = 1.0(-0.4)$, is the unity (maximum physical value) but it could be as low as 0.6.

Ion	C	$e^{-\tau}$	τ	N	$log\, N$
(1)	(2)	(3)	(4)	(5)	(6)
CIV	0.8 ± 0.1	0.4 ± 0.1	0.92 ± 0.25	$1.2 \pm 0.3\ (\times 10^{12}\, cm^{-2}/(km/s))$	12.08 ± 0.11
SiIV	$1.0(-0.4)$	0.6 ± 0.2	0.5 ± 0.3	$0.12 \pm 0.07\ (\times 10^{12}\, cm^{-2}/(km/s))$	11.08 ± 0.25

Table 4 Distances estimates for the absorber at $z \sim 2.457$ and in the range $\sim 10050 - \sim 10100$ km/s from the preliminary results given in Table 3. The columns give: (1) Logarithm of the ionisation fraction $log\, f$; (2) Logarithm of the ionisation parameter $log U$; (3) Ionisation parameter U; (4) Distance (assuming $n_e \sim 10^{15} m^{-3}$, a typical value for the BLR); (5) Distance (assuming $n_e \sim 10^{10} m^{-3}$, a typical value for the NLR).

$log\, f$	$log U$	U	R_{BLR}	R_{NLR}
(1)	(2)	(3)	(4)	(5)
2.01 ± 0.11	-1.2 ± 0.2	0.06 ± 0.04	19 ± 6 (pc)	5.9 ± 1.6 (kpc)

served in the sample. Radio observations of the radio BAL quasar sample will be needed to know whether the radio emission has a connection with the orientation of these outflows.

Acknowledgements FJL, IGS and CRB acknowledge financial support from the Spanish Ministerio de Educación y Ciencia under project AYA 2005-00055.

References

1. Adelman-McCarthy, J. K. et al. 2005, VizieR Online Data Catalog, 2267, 0
2. Adelman-McCarthy, J. K., Agüeros, M. A., Allam, S. S., Anderson, K. S. J., & 150 coauthors. 2007, ApJS, 172, 634
3. Arav, N., Becker, R. H., Laurent-Muehleisen, S. A., Gregg, M. D., White, R. L., Brotherton, M. S., & de Kool, M. 1999, ApJ, 524, 566 S. A., & Arav, N. 2000, ApJ, 538, 72
4. Becker, R. H., White, R. L., & Helfand, D. J. 1995, ApJ, 450, 559
5. Benn, C. R., Carballo, R., Holt, J., Vigotti, M., González-Serrano, J. I., Mack, K.-H., & Perley, R. A. 2005, MNRAS, 360, 1455
6. Carballo, R., Gonzalez-Serrano, J. I., Benn, C. R., & Jimenez-Lujan, F. 2008, ArXiv e-prints
7. Hall, P. B., Anderson, S. F., Strauss, M. A., York, D. G., Richards, G. T., Fan, X., Knapp, G. R., Schneider, D. P., Vanden Berk, D. E., Geballe, T. R., & 43 coauthors. 2002, ApJS, 141, 267
8. Hamann, F. 1997, ApJS, 109, 279
9. Hewett, P. C. & Foltz, C. B. 2003, AJ, 125, 1784
10. Korista, K. T., Voit, G. M., Morris, S. L., & Weymann, R. J. 1993, ApJS, 88, 357
11. Montenegro-Montes, F. M., Mack, K.-H., Vigotti, M., Benn, C. R., Carballo, R., González-Serrano, J. I., Holt, J., & Jiménez-Luján, F. 2008, MNRAS, 1853
12. Savage, B. D. & Sembach, K. R. 1991, ApJ, 379, 245
13. Weymann, R. J., Morris, S. L., Foltz, C. B., & Hewett, P. C. 1991, ApJ, 373, 23